Supporting Information

An efficient multi-doping strategy to enhance Li-ion conductivity in garnet-type solid electrolyte $Li_7La_3Zr_2O_{12}$

Yedukondalu Meesala,[a] Yu-Kai Liao,[b] Anirudha Jena,[ac] Nai-Hsuan Yang,[a] Wei Kong Pang,[d] Shu-Fen Hu,*[b] Ho Chang,*[c] Chia-Erh Liu,[e] Shih-Chieh Liao,[e] Jin-Ming Chen,[e] Xiangxin Guo*[f] and Ru-Shi Liu*[ab]

[a]*Department of Chemistry, National Taiwan University, Taipei 106, Taiwan*

[b]*Department of Physics, National Taiwan Normal University, Taipei 116, Taiwan*

[c]*Department of Mechanical Engineering and Graduate Institute of Manufacturing Technology, National Taipei University of Technology, Taipei 106, Taiwan*

[d]*Institute for Superconducting & Electronic Materials, University of Wollongong, NSW 2522, Australia*

[e]*Material and Chemical Research Laboratories, Industrial Technology Research Institute, Hsinchu 300, Taiwan*

[f]*College of Physics, Qingdao University, Qingdao 266071, China*

AUTHOR INFORMATION

***Corresponding authors**

E-mails: rsliu@ntu.edu.tw (R. S. Liu)

f10381@ntut.edu.tw (H. Chang)

sfhu.hu@gmail.com (S. F. Hu)

xxguo@qdu.edu.cn (X. Guo)

Table S1. XRD refined atomic occupation factors, fractional coordinates, and isotropic thermal factors of the undoped LLZO, mono-doped LLZTO, dual-doped LLBZTO, and ternary-doped LGLBZTO.

Garnet	***GOF***	R_{wp}	***atom***	***site***	***Occupancy***	***X***	***y***	***z***	U_{iso}**/(Å)**
LLZO	1.77	10.36%	Li	*24d*	0.32*	0.375	0	0.25	0.021(1)
			Li	*96h*	0.36*	0.094(2)	0.685(2)	0.585(3)	0.021(1)
			Al	24*d*	0.06	3/8	0	1/4	0.01
			La	*24c*	1	0.125	0	0.25	0.0108(6)
			Zr	*16a*	1	0	0	0	0.00075(7)
			O	*96h*	1	0.9724(3)	0.0551(6)	0.1487(4)	0.0107(4)
LLZTO	2.34	8.86%	Li	*24d*	0.52*	0.375	0	0.25	0.14(4)
			Li	*96h*	0.33*	0.697(5)	0.599(5)	0.079(5)	0.09(4)
			La	*24c*	1	0.125	0	0.25	0.0014(5)
			Zr	*16a*	0.875**	0	0	0	0.0035(3)
			Ta	*16a*	0.125**	0	0	0	0.0015(3)
			O	*96h*	1	0.9724(7)	0.0651(7)	0.1426(7)	0.0107(4)
LLBZTO	2.20	9.92%	Li	*24d*	0.65*	0.375	0	0.25	0.20(7)
			Li	*96h*	0.33*	0.651(4)	0.599(4)	0.047(4)	0.20(5)
			La	*24c*	0.9833**	0.125	0	0.25	0.0014(5)
			Ba	*24c*	0.0167**	0.125	0	0.25	0.0014(5)
			Zr	*16a*	0.875**	0	0	0	0.0035(3)
			Ta	*16a*	0.125**	0	0	0	0.0015(3)
			O	*96h*	1	0.9724(7)	0.05919(7)	0.13992(7)	0.0107(4)
LGLBZTO	2.37	10.82%	Li	*24d*	0.77*	0.375	0	0.25	0.20(5)
			Li	*96h*	0.33*	0.7342(4)	0.5961(4)	0.055(4)	0.18(5)
			Ga	*24d*	0.0598(5)	0.375	0	0.25	0.20(7)
			La	*24c*	0.9833**	0.125	0	0.25	0.0014(5)
			Ba	*24c*	0.0167**	0.125	0	0.25	0.0014(5)
			Zr	*16a*	0.875**	0	0	0	0.0035(3)
			Ta	*16a*	0.125**	0	0	0	0.0015(3)
			O	*96h*	1	0.9731(9)	0.05726(9)	0.13875(9)	0.006(3)

* From neutron data **fixed

Table S2. The d(0.1), d(0.5), and d(0.9) values of undoped LLZO mono-doped LLZTO, dual-doped LLBZTO, and ternary-doped LGLBZTO.

Garnet	d(0.1)	d(0.5)	d(0.9)	*Span
LLZO	2.217 μm	2.734 μm	5.007 μm	1.02 μm
LLZTO	0.506 μm	3.493 μm	6.102 μm	1.60 μm
LLBZTO	0.538 μm	3.668 μm	7.926 μm	2.01 μm
LGLBZTO	0.553 μm	3.68 μm	8.138 μm	2.06 μm

$$*Span = \frac{D_{v0.9} - D_{v0.1}}{D_{v0.5}}$$

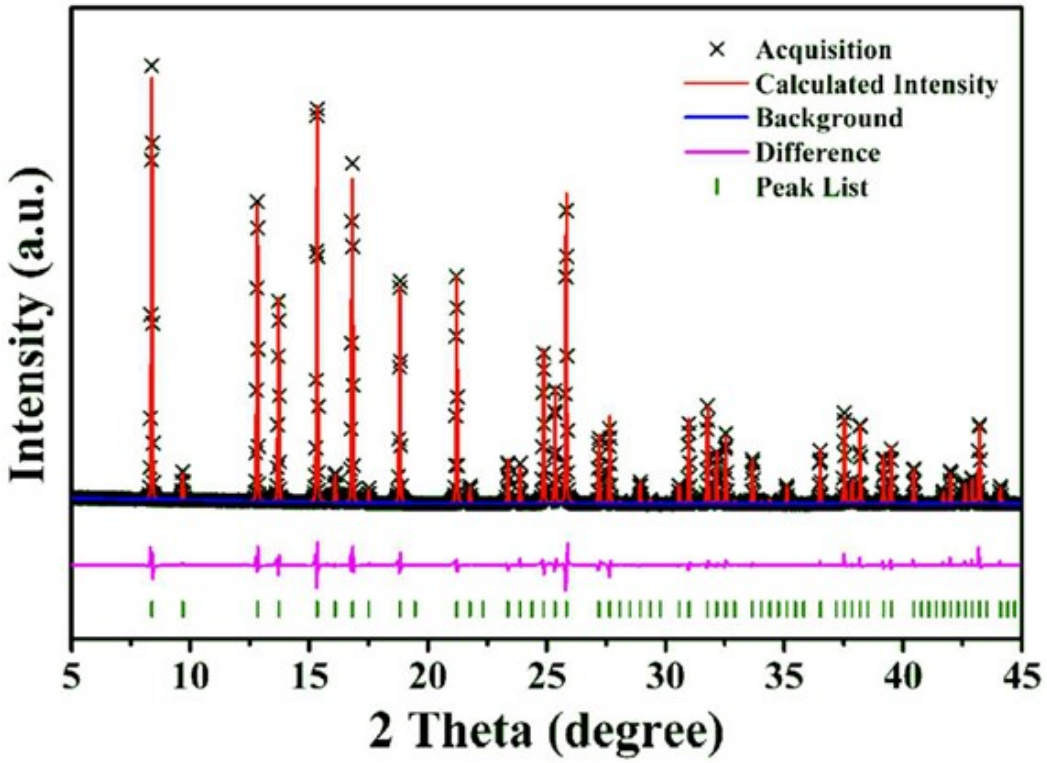

Fig. S1 Rietveld analysis of Synchrotron X-ray powder diffraction pattern of the undoped LLZO; observed (crosses), calculated, and difference profiles; vertical bars correspond to the calculated Bragg reflections for cubic garnet.

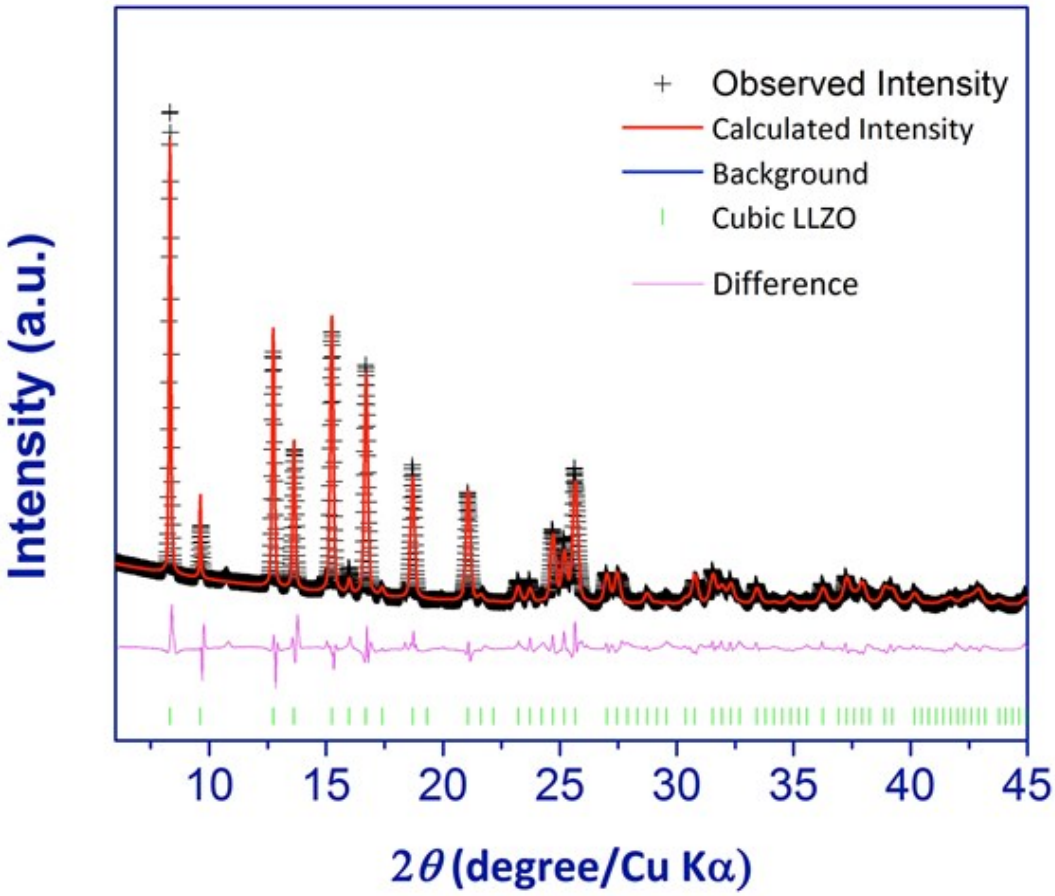

Fig. S2 Rietveld analysis of Synchrotron X-ray powder diffraction pattern for the mono-doped LLZTO; observed (crosses), calculated, and difference profiles; vertical bars correspond to the calculated Bragg reflections for cubic garnet.

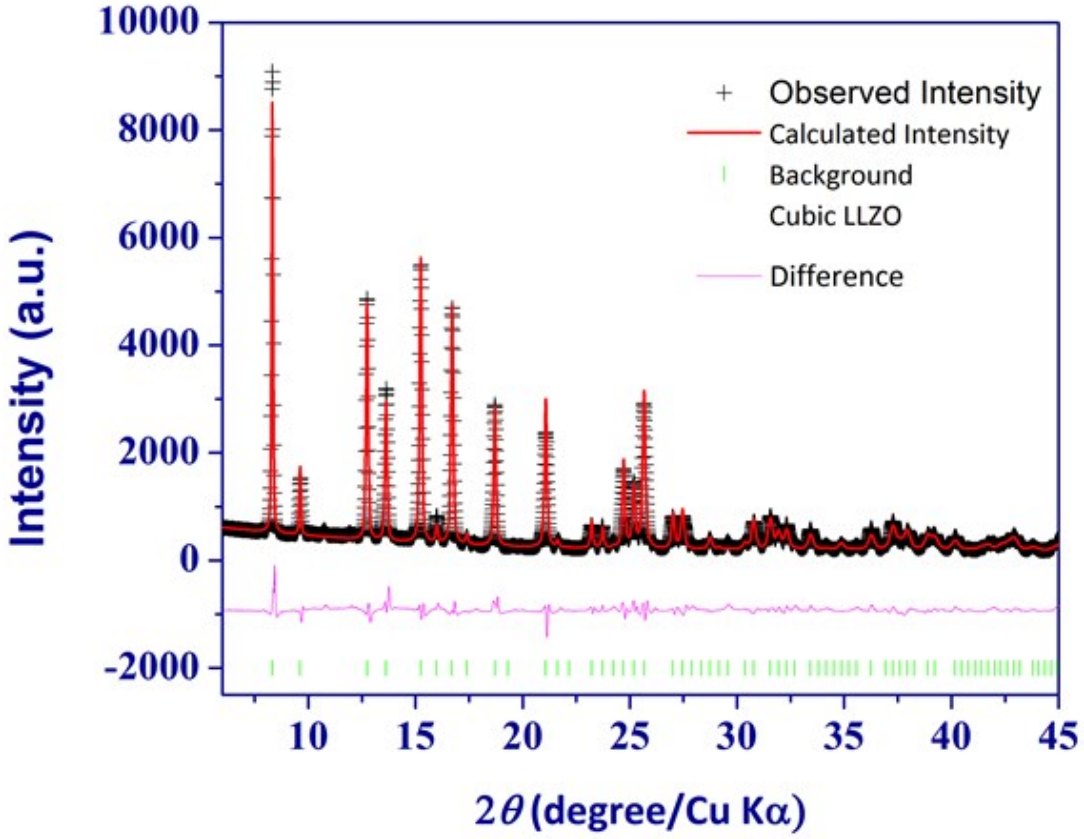

Fig. S3 Rietveld analysis of Synchrotron X-ray powder diffraction pattern for the dual-doped LLBZTO; observed (crosses), calculated, and difference profiles; vertical bars correspond to the calculated Bragg reflections for cubic garnet.

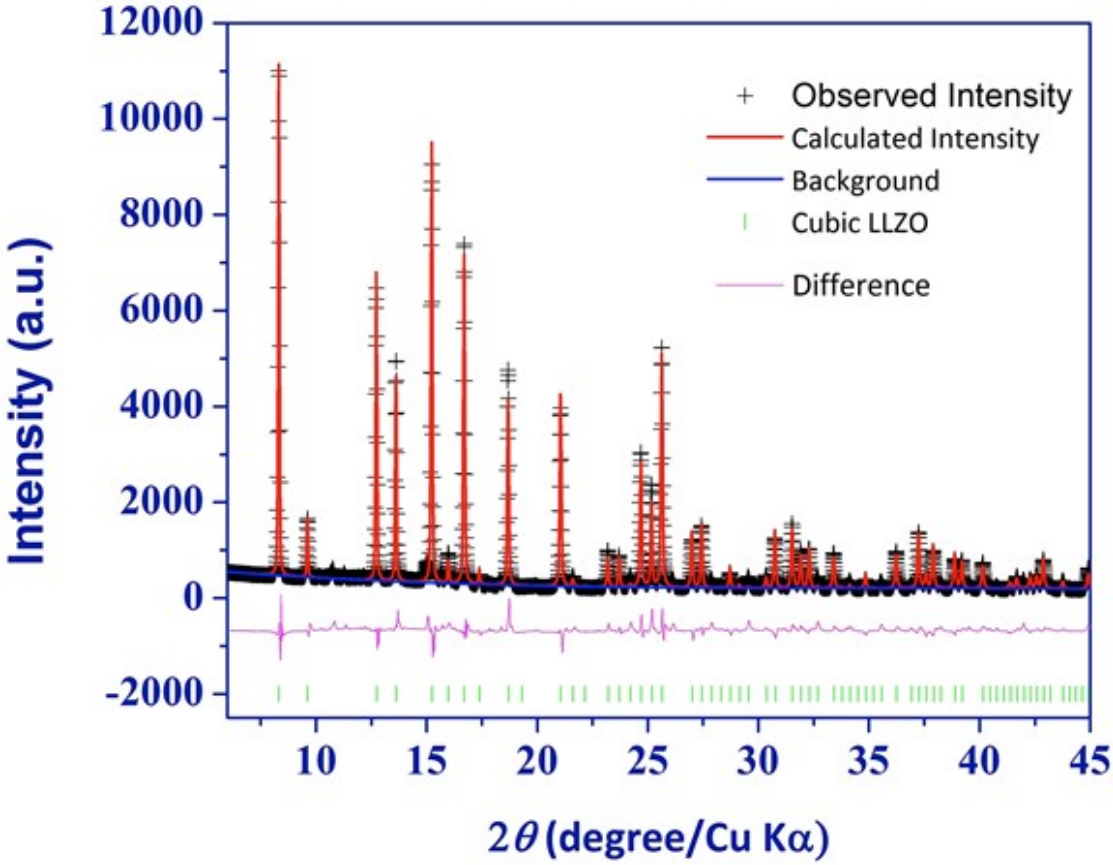

Fig. S4 Rietveld analysis of Synchrotron X-ray powder diffraction pattern for the ternary-doped LGLBZTO; observed (crosses), calculated, and difference profiles; vertical bars correspond to the calculated Bragg reflections for cubic garnet.

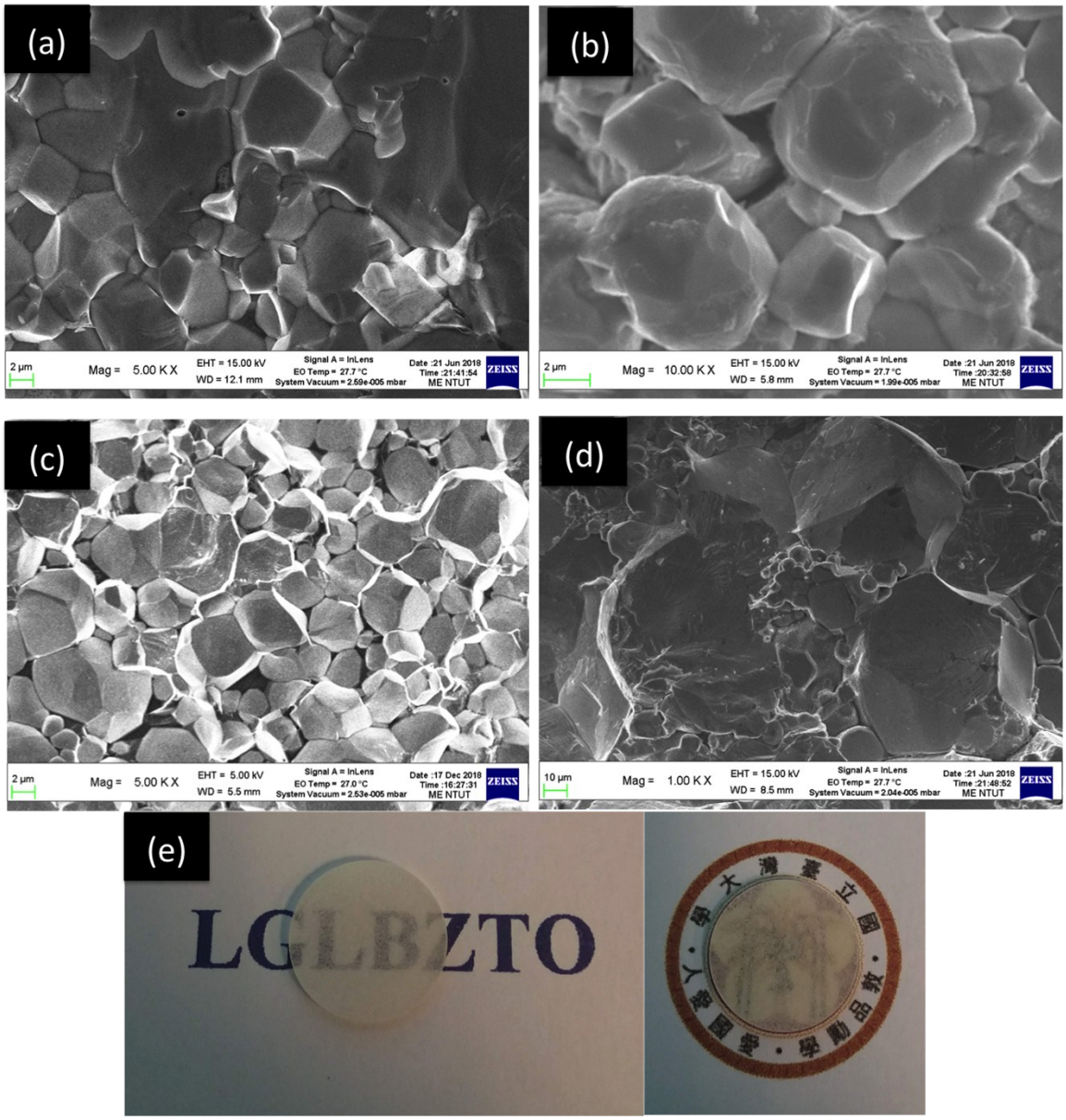

Fig. S5 FE-SEM images of the (a) undoped LLZO, (b) mono-doped LLZTO, (c) dual-doped LLBZTO, and (d) ternary-doped LGLBZTO (e) Optical photographs of LGLBZTO with 0.5mm thickness.

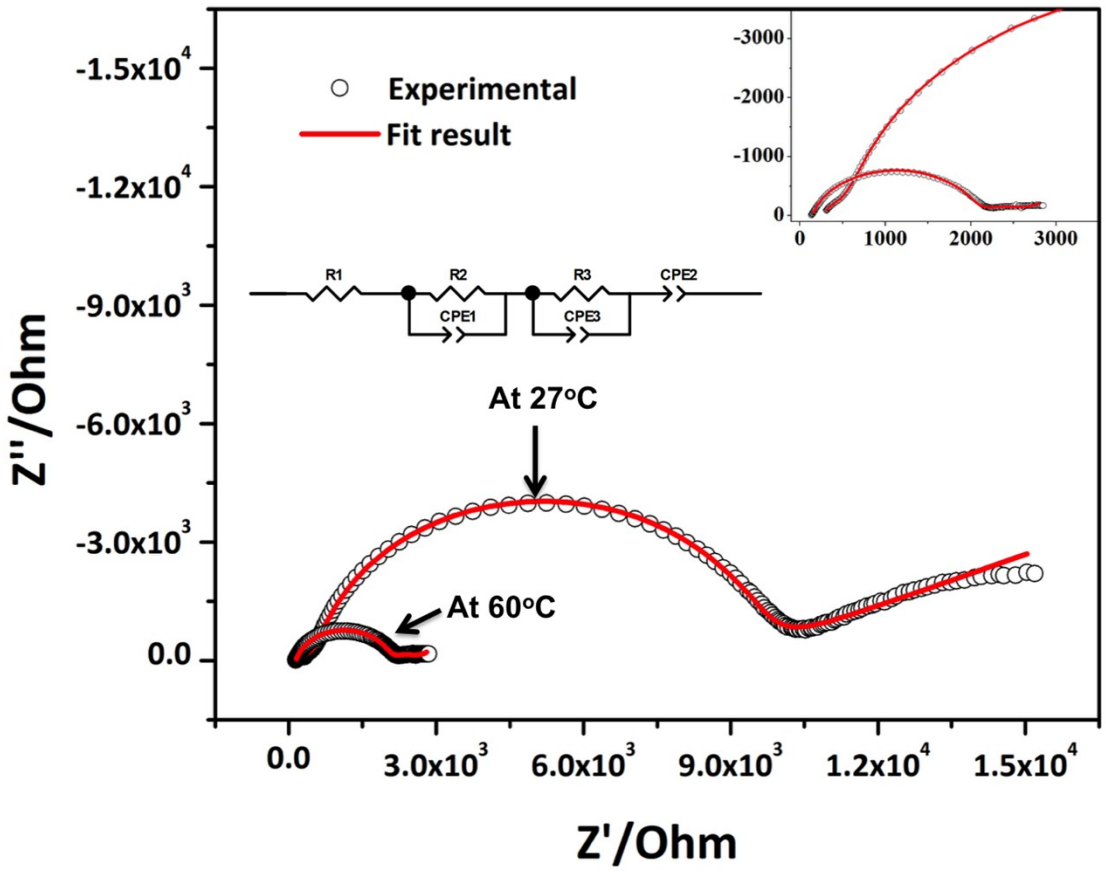

Fig. 6 Impedance spectra of the symmetrical cell Li|LGLBZTO|Li measured at 27 and 60 °C.

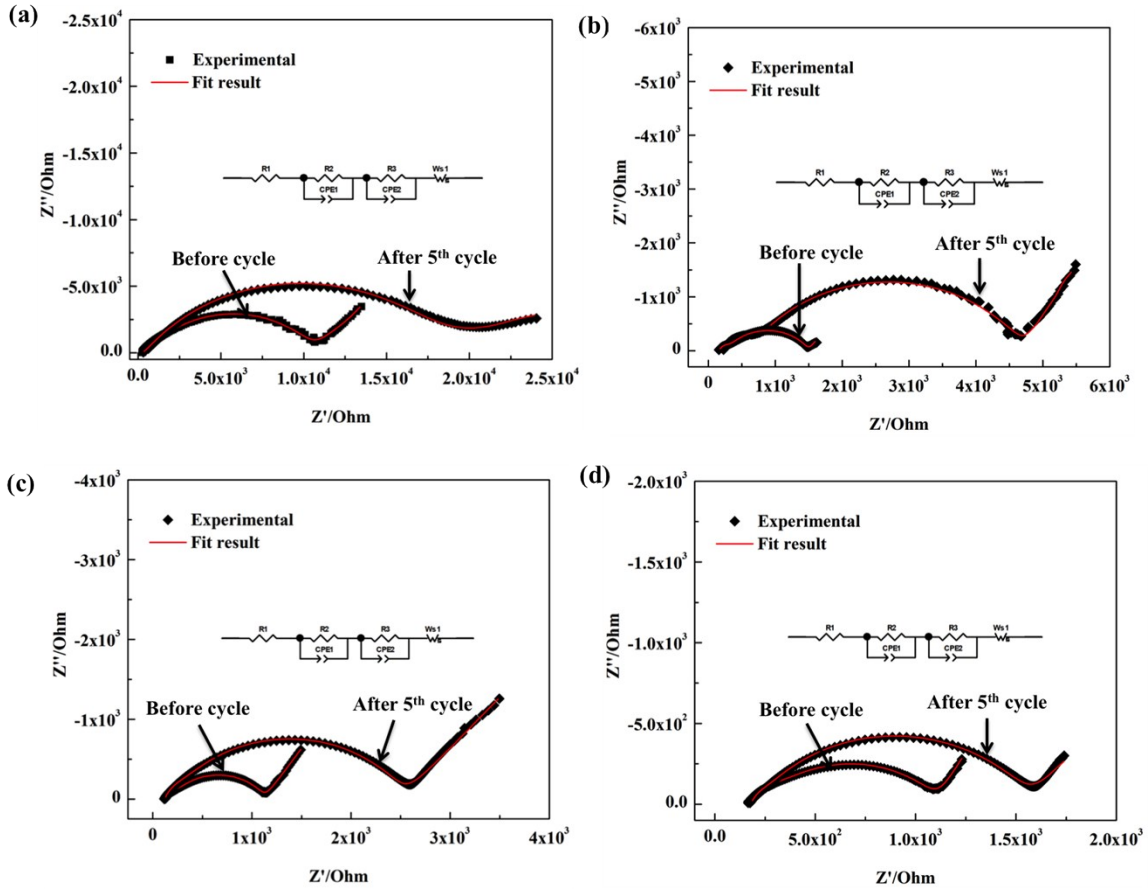

Fig. 7 Impedance spectra of the symmetrical cell with the configuration of (a) Li|LLZO|LFP (b) Li|LLZTO|LFP (c) Li|LLBZTO|LFP and (d) Li|LGLBZTO|LFP recorded before and after 5th cycle at 60 °C.